

Spectral and kinetic properties of the radical ions of chloroboron(III) subnaphthalocyanine

Noemí Rubio^a, Ana Jiménez-Banzo^a, Tomás Torres^b, Santi Nonell^{a,*}

^a Grup d'Enginyeria Molecular, Institut Químic de Sarrià, Universitat Ramon Llull, Via Augusta 390, 08017 Barcelona, Spain

^b Department of Organic Chemistry C-I, Universidad Autónoma de Madrid, Cantoblanco, 28049 Madrid, Spain

Received 3 March 2006; received in revised form 9 June 2006; accepted 14 June 2006

Available online 1 August 2006

Abstract

Both the radical anion and radical cation of the chloroboron(III) subnaphthalocyanine (SubNc) cone-shaped macrocycle have been photochemically produced and their kinetics and absorption spectra have been characterised. SubNc is more prone to oxidation but less prone to reduction than its higher homologue, the chloroaluminium(III) phthalocyanine (Pc). Given the higher triplet quantum yield of SubNc compared to Pc, SubNc emerges as a very good photosensitiser for triplet-mediated reduction processes. The radical-ion spectra follow the same patterns found for Pcs, namely absorption bands at longer wavelengths than those of the singlet and triplet excited states.

© 2006 Elsevier B.V. All rights reserved.

Keywords: Absorption spectra; Radical ions; Redox potentials; Subnaphthalocyanines

1. Introduction

Porphyrinoid macrocycles absorbing in the visible and near-IR spectral region are the subject of an intensive research for potential for solar energy conversion [1–3], non-linear optical materials [4–6], organic light-emitting diodes [7,8], conducting polymers [9], and biomedical applications such as the photodynamic therapy of tumours (PDT) [10–14]. For such applications, understanding the excited-state properties and reactivity is essential. Of particular interest is the photochemical production of radical ions, e.g. in photoinduced electron transfer reactions, aiming at mimicking the natural photosynthesis [15] or for the oxidation of biological substrates in PDT.

Subphthalocyanines (SubPcs) and subnaphthalocyanines (SubNcs, Fig. 1) are novel lower homologues of phthalocyanines

(Pc) and naphthalocyanines (Nc), respectively, which show the remarkable properties of a non-planar conical shape [16,17]. In a previous work [18], we reported on the basic photophysics of the SubNc macrocycle. SubNc shows a fluorescence quantum yield (Φ_F) of 0.22, a value very similar to that found for related SubPcs ($\Phi_F = 0.25$) [19] and naphthalocyanines ($\Phi_F = 0.20$ for aluminium naphthalocyanine tetrasulfonate (AlNcS₄) [20]), but three-fold lower than that for phthalocyanines, e.g., $\Phi_F = 0.58$ for chloroaluminium phthalocyanine (AlPcCl) [21]. Conversely, the triplet (Φ_T) and singlet oxygen quantum yields (Φ_Δ) of SubNc are 0.68, similar to those of SubPc ($\Phi_T = 0.62$; $\Phi_\Delta = 0.61$) [19], but remarkably higher than those of AlPcCl ($\Phi_T = 0.4$ [21]), of its sulfonic acid derivatives ($\Phi_\Delta = 0.36$ [22]) and of bis(tri-*n*-hexylsiloxy)silicon 2,3-naphthalocyanine (SiNc, $\Phi_T = 0.20$; $\Phi_\Delta = 0.19$ [23]).

Given their potential application in photo-induced electron transfer processes, we report now on the electrochemistry, photochemical production, and kinetic and spectral characterisation of both the radical anion and radical cation of SubNc.

2. Materials and methods

2.1. Chemicals

SubNc was synthesised as described previously [18]. Biphenyl (BP, 99%), benzonitrile (PhCN, 99.9%, HPLC

Abbreviations: AlNcS₄, aluminium naphthalocyanine tetrasulfonate; AlPcCl, chloroaluminium phthalocyanine; BP, biphenyl; CV, cyclic voltammetry; DMF, dimethylformamide; HFP, 1,1,1,3,3,3-hexafluoropropan-2-ol; MA⁺, *N*-methylacridinium hexafluorophosphate; Pc, phthalocyanine; PDT, photodynamic therapy; PhCN, benzonitrile; SiNc, bis(tri-*n*-hexylsiloxy)silicon 2,3-naphthalocyanine; SubNc, subnaphthalocyanine; SubPc, chloroboron subphthalocyanine; TBAHP, tetrabutylammonium hexafluorophosphate; TMPD, *N,N,N',N'*-tetramethyl-*p*-phenylenediamine

* Corresponding author. Tel.: +34 93 267 20 00; fax: +34 93 205 62 66.

E-mail address: s.nonell@iqs.edu (S. Nonell).

grade) and 1,1,1,3,3,3-hexafluoropropan-2-ol (HFP, 99.9%) were all purchased from Aldrich and used as received. *N,N,N',N'*-tetraphenyl-*p*-phenylenediamine (TMPD, 99%) was from Sigma. Dimethylformamide (DMF) was purchased from SDS and was dried over 4 Å molecular sieves. Tetrabutylammonium hexafluorophosphate (TBAHP) electrochemical grade was purchased from Fluka. *N*-Methylacridinium hexafluorophosphate (MA⁺) was synthesised by methylation of acridine with methyl iodide in refluxing acetonitrile followed by treatment of the resulting MA⁺ iodide with silver hexafluorophosphate in methanol [24]. Nitrogen 5.0 and argon 5.0 were from Abelló-Linde.

2.2. Electrochemical and photophysical measurements

Cyclic voltammetry (CV) measurements were performed using a cylindrical cell with a 0.093 cm² platinum sphere as the work electrode, a platinum wire as the counter-electrode, and a Ag/AgCl 3.5 M as the reference electrode. DMF solutions containing SubNc (1 mM) and TBAHP (0.1 M), as the supporting electrolyte, were purged with nitrogen for 20 min prior to experiment. The scan speed was set to 100 mV s⁻¹.

Absorption spectra were recorded on a Varian Cary 4 spectrophotometer. Radicals were produced and characterised with a home-made nanosecond laser flash photolysis apparatus using an OPO laser (SL OPO, Continuum; 5 ns pulsewidth, 1–10 mJ per pulse) pumped by a Q-switched Nd-YAG laser (Surelite I-10, Continuum) for excitation. Photoinduced absorbance changes were monitored at 90° by an analysing beam produced by a Xe lamp (PTI, 75W) in combination with a dual-grating monochromator (mod.101, PTI) coupled to a photomultiplier (Hamamatsu R928) for 300–800 nm detection and a North Coast EO-817P germanium detector for 800–1600 nm (Fig. 1).

Kinetic analysis of the individual transients was done with the software FitLW developed in our group. Global kinetic analysis of the generated transient time–absorbance–wavelength matrix

was performed with the software Specfit (Spectrum Software Associates). All measurements were carried out in PhCN or in mixtures HFP:PhCN (9:1).

3. Results and discussion

3.1. Electrochemical properties

The first oxidation and reduction half-wave potentials of the SubNc have been measured by CV (Fig. 2).

SubNc shows a quasi-reversible reduction at the potential $E_{1/2}(S/S^{\bullet-}) = -0.85$ V versus Ag/AgCl. SubNc is easier to reduce than its subphthalocyanine counterpart (-1.05 V versus Ag/AgCl for SubPc [19]), but more difficult to reduce than the phthalocyanine AlPcCl whose reduction potential is $E^0 = 0.64$ V versus Ag/AgCl [21].

In contrast, the oxidation of SubNc in DMF takes place irreversibly at $E_{1/2}(S^{\bullet+}/S) \approx 0.68$ V versus Ag/AgCl. It is accompanied by the disappearance of the cathodic peak, probably reflecting that electron transfer is followed by a chemical reaction [25]. SubNc is more prone to oxidation than the SubPc homologue (1.04 V versus Ag/AgCl [19]) and than AlPcCl (0.96 V versus Ag/AgCl [21]). Overall, these results are consistent with a stabilisation of the LUMO and a significant destabilisation of the HOMO in SubNc relative to SubPc, as is found in the Pc series [26].

For photoinduced electron transfer processes, the relevant redox potentials are those of the excited states. They are calculated by adding (for reduction) or subtracting (for oxidation) the excited-state energy to the ground-state potentials (Table 1). We used 1.85 eV for the energy of the first excited singlet state, calculated from the intersection point of the normalised absorption and fluorescence spectra. Since no phosphorescence could be detected for SubNc even at 77 K, the energy of T_1 (1.35 eV [18]) was estimated by the method of Dreeskamp et al. from fluorescence quenching by 1-iodopropane [27].

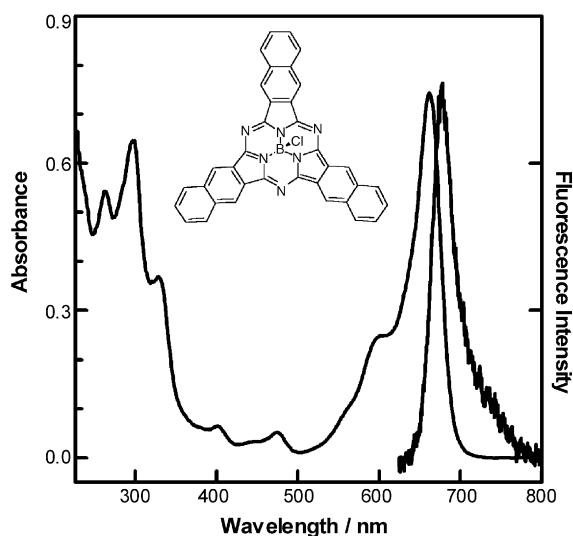


Fig. 1. Absorption and fluorescence spectra of SubNc in dichloromethane and toluene, respectively.

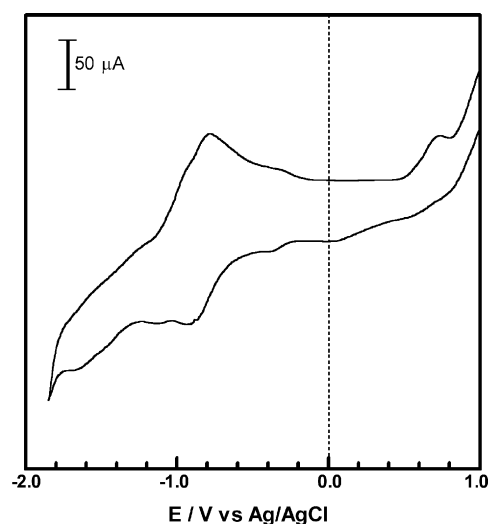


Fig. 2. Cyclic voltammogram of the SubNc in nitrogen-saturated DMF containing 0.1 M TBAHP. Sweep rate: 100 mV s⁻¹ [SubNc] = 1 mM.

Table 1
Ground- and excited-state redox potentials of SubNc in DMF

	Ground state	Singlet excited state ^a	Triplet excited state ^b
$E(S/S^{\bullet-})^c$			
SubNc	-0.85	+1.00	+0.50
SubPc	-1.05	+1.12	+0.40
AlPcCl	-0.64	+1.16	+0.56
$E(S^{\bullet+}/S)^d$			
SubNc	+0.68	-1.17	-0.67
SubPc	+1.04	-1.13	-0.41
AlPcCl	+0.96	-0.84	-0.24

Values for subphthalocyanine [19] and [21] are given for comparison.

^a E_S (SubNc)=1.85 eV [18]; E_S (SubPc)=2.17 eV [19]; E_S (AlPcCl)=1.80 eV [21].

^b E_T (SubNc)=1.35 eV [18]; E_T (SubPc)=1.45 eV (see supporting information); E_T (AlPcCl)=1.20 eV [21].

^c Excited-state potentials calculated as $E(S/S^{\bullet-}) + E^*$.

^d Excited-state potentials calculated as $E(S/S^{\bullet-}) - E^*$.

While the excited-state reduction of SubNc occurs at similar potentials to those of SubPc and Pc, the oxidation of SubNc is more favourable, particularly in the triplet state. Given the higher triplet quantum yield of SubNc compared to Pc, SubNc emerges as a very good photosensitiser for triplet-mediated reduction processes.

3.2. Radical anion production and characterisation

The radical anion of the SubNc was produced by photoinduced electron transfer from TMPD, which has an oxidation potential low enough ($E^0(\text{TMPD}^{\bullet+}/\text{TMPD})=0.20$ V versus Ag/AgCl in PhCN) [28–30] to reduce the triplet state of SubNc. Thus, the triplet lifetime of SubNc decreases in the presence of TMPD according to $1/\tau = (1/\tau_0) + k_q [\text{TMPD}]$ (Fig. 3), where τ_0 and τ are the triplet lifetimes in the absence and in the presence of TMPD, respectively.

From the slope of the linear relationship in Fig. 3, SubNc^{•-} is formed with an observed rate constant of $(1.95 \pm 0.06) \times 10^9 \text{ M}^{-1} \text{ s}^{-1}$ in PhCN, which is near to the diffusion-control value [31].

For the characterisation of the transient absorption spectrum and kinetics of SubNc^{•-}, a benzonitrile solution containing SubNc and TMPD (50 μM) was photoexcited at 660 nm. Transient absorption spectra at different time delays after the laser pulse shows the presence of ³SubNc, SubNc^{•-}, and TMPD^{•+} (³SubNc and TMPD^{•+} identified by similarity to the published spectra [18,32,33]; see also the electronic supplementary information). Global analysis of the time-absorbance-wavelength matrix afforded the spectrum assigned to ³SubNc and SubNc^{•-} as well as their kinetics (Fig. 4 and the supporting information).

SubNc^{•-} lives 350 μs in deaerated PhCN. The spectra of ³SubNc and SubNc^{•-} are remarkably similar, though a number of differences are worth noting. In the NIR region, SubNc^{•-} shows a sharp band at 750 nm together with a less-intense broadband with maximum at 830 nm. ³SubNc shows only one sharp band at 715 nm. In the UV-vis region, SubNc^{•-} shows wide

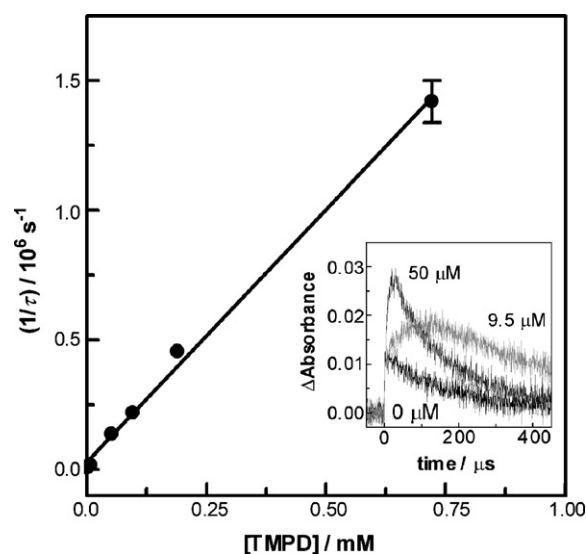


Fig. 3. Quenching of ³SubNc lifetime by TMPD in argon-saturated PhCN. Inset: Transient decays at different TMPD concentrations; $\lambda_{\text{exc}}=660$ nm, $\lambda_{\text{obs}}=550$ nm. [TMPD]=0 μM , $\tau=179 \pm 8 \mu\text{s}$; [TMPD]=9.5 μM , τ (rise)= $62 \pm 4 \mu\text{s}$, τ (decay)= $402 \pm 4 \mu\text{s}$; [TMPD]=50 μM , τ (rise)= $7.3 \pm 1 \mu\text{s}$, τ (decay)= $153 \pm 2 \mu\text{s}$; [TMPD]=95 μM , τ (rise)= $4.0 \pm 0.5 \mu\text{s}$, τ (decay)= $149 \pm 2 \mu\text{s}$; [TMPD]=190 μM , τ (rise)= $2.0 \pm 0.2 \mu\text{s}$, τ (decay)= $136 \pm 2 \mu\text{s}$; [TMPD]=722 μM , τ (rise)= $0.70 \pm 0.02 \mu\text{s}$, τ (decay)= $130 \pm 5 \mu\text{s}$.

absorption bands with peaks at 550 and 360 nm. The latter is a specially good marker because ³SubNc shows bleaching of the ground state.

The transient absorption spectrum of SubNc^{•-} is very similar to that reported for (dodecafluorosubphthalocyanato)-chloroboron(III) (SubPcF₁₂) in acetonitrile [34], which shows bands at 490 and 750 nm. A similar pattern is typically observed for the parent Pc [35–38]: two prominent absorption bands in the regions 570–580 and 635–645 nm, with two weaker bands occurring at 320–430 and 960–970 nm. By analogy to Pcs, we tentatively assign the bands at 750 nm to the Q transitions, that

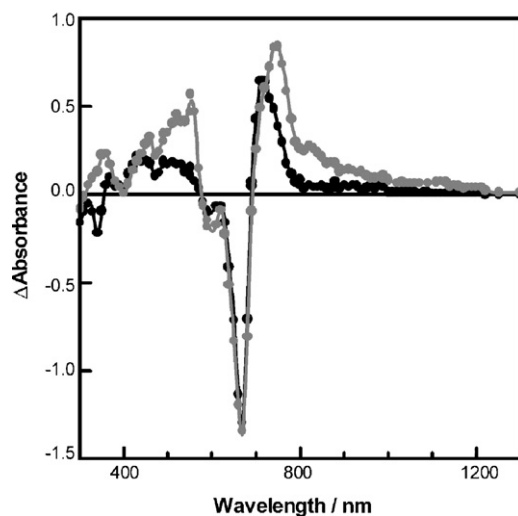


Fig. 4. Transient absorption spectrum of ³SubNc (black) and of SubNc^{•-} (grey) as recovered by global analysis of the time-absorbance-wavelength matrix. [SubNc]=2.7 μM .

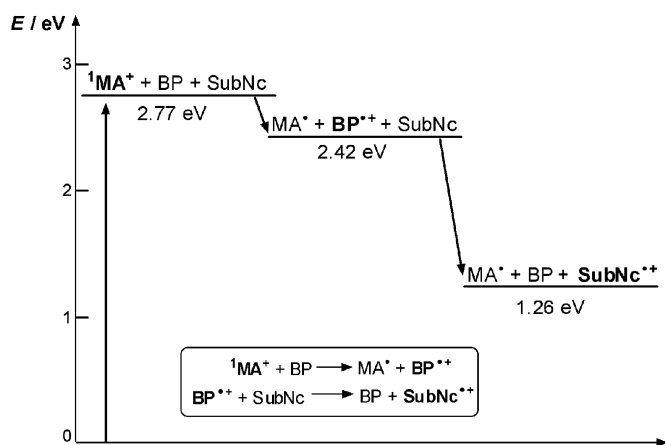
at 550 nm to $\pi-\pi^*$ transitions, and that at 360 nm to B1/B2 transitions [36].

3.3. Radical cation production and characterisation

The radical cation was also produced photochemically using the cosensitisation method [39–45]. A photoexcited primary electron acceptor ($^1\text{MA}^+$, $E(^1\text{MA}^+/\text{MA}^\bullet) = 2.35$ V versus Ag/AgCl in CH_2Cl_2 [46]) abstracts an electron from a cosensitiser (BP, $E(\text{BP}^{\bullet+}/\text{BP}) = 2.00$ V versus Ag/AgCl in CH_2Cl_2 [43]), producing its long-lived radical cation ($\text{BP}^{\bullet+}$). This species subsequently abstracts an electron from SubNc to yield its radical cation (Scheme 1). As this is formally a charge-shift process, separation of the product pair is not precluded by electrostatic interaction.

SubNc $^{\bullet+}$ was thus produced by the 450-nm excitation of a solution containing MA^+ (1 mM), BP (0.2 M) and SubNc (40 μM) in either PhCN or HFP containing 10% PhCN. Under these conditions, less than 10% of the incoming photons are absorbed by SubNc. HFP is a solvent of very weak nucleophilicity, high hydrogen bonding donor strength, low hydrogen bonding acceptor strength, high polarity ($\epsilon \sim 300$), and high ionising power. These properties make HFP an ideal solvent for reactions where stabilisation of radical cations is required or where anion participation is not desirable [47–49]. We have shown that this solvent is very convenient for photochemical production of radical cations of porphyrinoid macrocycles. Electron-transfer reaction SubNc to $\text{BP}^{\bullet+}$ occurs with a rate constant of $1.6 \times 10^{10} \text{ M}^{-1} \text{ s}^{-1}$ in PhCN, and $3.2 \times 10^{10} \text{ M}^{-1} \text{ s}^{-1}$ in HFP. All these rate constants are near the diffusion-control limit, indicating an effective radical-cation generation.

The transient absorption spectra at different time delays after the laser pulse shows the presence of MA^\bullet , $\text{BP}^{\bullet+}$ and SubNc $^{\bullet+}$ (MA^\bullet , $\text{BP}^{\bullet+}$ identified by similarity to the published spectra [45]; see also the electronic supplementary information). Global analysis of the time–absorbance–wavelength matrix afforded the spectrum of all the species involved in this photosystem as well as their kinetics (see supporting information). Fig. 5 shows the transient absorption spectra of SubNc $^{\bullet+}$, in both PhCN and HFP.



Scheme 1. Energy diagram showing the cascade of events leading to the formation of SubNc $^{\bullet+}$ by the co-sensitisation method [43,46,54].

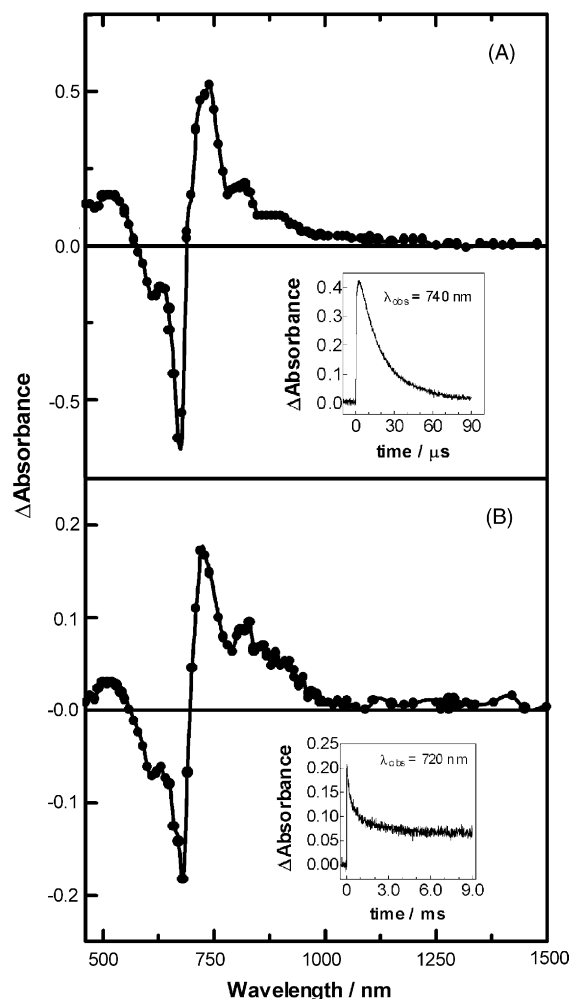


Fig. 5. Transient absorption spectra of SubNc $^{\bullet+}$ in (A) PhCN and (B) HFP, as recovered by global analysis of the time–absorbance–wavelength matrix. Insets: Transient decay of SubNc $^{\bullet+}$. [SubNc] = 40 μM .

SubNc $^{\bullet+}$ lives 30 μs in PhCN and more than 8 ms in HFP, above the time window of our set-up (Fig. 5, Insets), confirming the stabilisation effect observed previously [45].

The transient absorption spectrum of SubNc $^{\bullet+}$ in PhCN shows a broad band in the 460–570 nm region, centred on 520 nm and in the NIR region peaking at 740 and 820 nm (Fig. 5A). Transient absorption below 460 nm was dominated by the intense photobleaching of the MA^+ ground state.

In HFP, SubNc $^{\bullet+}$ also shows a broadband in the 460–570 nm region centred on 510 and 10 nm hypsochromically shifted with regard to that in PhCN, and in the NIR region with maxima at 720 and 20 nm hypsochromically shifted respect to that in PhCN, and at 830 nm. The hypsochromic shift can be attributed to the ability of the protic solvents to form hydrogen bonds with lone pairs of the nitrogen in the macrocycle. Thus the energy of the π -state is lowered without modifying the π^* -state, i.e., ground state energy stabilises, as it is found in other tetrapyrrolic macrocycles [50].

Gonzalez-Rodriguez et al. published the differential absorption spectrum of the radical cation of a substituted SubPc in the range 500–960 nm [51]. The shape of its spectrum is very similar

to that of the SubNc^{•+} but hipsochromically shifted. Absorption spectra of the radical cations of the phthalocyanines follow similar tendencies: two NIR bands around 720 and 825 nm, a wide band centred at 500–510 nm, and an intense UV-band around 320 nm [52,53]. By analogy to Pcs, we tentatively assign the bands at 740 and 820 nm to the Q transitions, and that at 520 nm to n– π transitions [36].

4. Conclusions

This work describes the features of the radical ion forms of SubNc. This cone-shaped macrocycle is more prone to oxidation – but less to reduction – than its higher homologue, the phthalocyanine (Pc) ring. Given the higher triplet quantum yield of SubNc compared to Pc, SubNc emerges as a very good photosensitiser for triplet-mediated reduction processes. Spectroscopically, the spectra of the radical ions of SubNc follow the π -radical pattern found in phthalocyanines and subphthalocyanines, i.e., absorption bands at longer wavelengths than those of the singlet and triplet excited states, which in turn reflect smaller energy gaps within bonding or non-bonding states in relation to the energy gap between bonding and nonbonding states.

These spectral patterns should allow to ascertain the participation and role of the radical ions of SubNc in photo-induced processes such as artificial photosynthesis or photodynamic therapy.

Acknowledgements

N.R. and A.J.-B. thank the Fundació Patronat Institut Químic de Sarrià and the Generalitat de Catalunya (DURSI), respectively for granting their predoctoral fellowships. Financial support by the Spanish MCyT is gratefully acknowledged (Grant No. SAF2002-04034-C02-02).

Appendix A. Supplementary data

Supplementary data associated with this article can be found, in the online version, at doi:10.1016/j.jphotochem.2006.06.007.

References

- [1] D. Gonzalez-Rodriguez, T. Torres, Proc. Electrochem. Soc. 12 (2002) 195–210.
- [2] M.E. El-Khouly, O. Ito, P.M. Smith, F. D'Souza, J. Photochem. Photobiol. C: Rev. 5 (2004) 79–104.
- [3] W.M. Campbell, A.K. Burrell, D.L. Officer, K.W. Jolley, Coord. Chem. Rev. 248 (2004) 1363–1379.
- [4] G. de la Torre, T. Torres, F. Agulló-López, Adv. Mater. 9 (1997) 265–269.
- [5] G. de la Torre, P. Vázquez, F. Agulló-López, T. Torres, Chem. Rev. 104 (2004) 3723–3750.
- [6] M. Calvete, G.Y. Yang, M. Hanack, Synth. Met. 141 (2004) 231–243.
- [7] D. Hohnholz, S. Steinbrecher, M. Hanack, J. Mol. Struct. 521 (2000) 231–237.
- [8] W.H. Flora, H.K. Hall, N.R. Armstrong, J. Phys. Chem. B 107 (2003) 1142–1150.
- [9] K.S. Suslick, N.A. Rakow, M.E. Kosal, J.-H. Chou, J. Porphyrins Phthalocyanines 4 (2000) 407–413.
- [10] E.D. Sternberg, D. Dolphin, C. Brückner, Tetrahedron 54 (1998) 4151–4202.
- [11] M.G.H. Vicente, Curr. Med. Chem. Anti-Cancer Agents 1 (2001) 175–194.
- [12] E.S. Nyman, P.H. Hynninen, J. Photochem. Photobiol. B: Biol. 73 (2004) 1–28.
- [13] S.K. Pushpan, S. Venkatraman, V.G. Anand, J. Sankar, D. Parmeswaran, S. Ganesan, T.K. Chandrashekar, Curr. Med. Chem. Anti-Cancer Agents 2 (2002) 187–207.
- [14] M.R. Detty, S.L. Gibson, S.J. Wagner, J. Med. Chem. 47 (2004) 3897–3915.
- [15] D. Gust, T.A. Moore, Adv. Photochem. 16 (1991) 1–65.
- [16] C.G. Claessens, D. Gonzalez-Rodriguez, T. Torres, Chem. Rev. 102 (2002) 835–853.
- [17] T. Torres, Angew. Chem. Int. Ed. 45 (2006) 2834–2837.
- [18] S. Nonell, N. Rubio, B. del Rey, T. Torres, J. Chem. Soc., Perkin Trans. 2 (2000) 1091–1094.
- [19] B. del Rey, U. Keller, T. Torres, G. Rojo, F. Agulló-López, S. Nonell, C. Martí, S. Brasselet, I. Ledoux, J. Zyss, J. Am. Chem. Soc. 120 (1998) 12808–12817.
- [20] I. McCubbin, D. Phillips, J. Photochem. 34 (1986) 187–195.
- [21] J.R. Darwent, P. Douglas, A. Harriman, G. Porter, M.C. Richoux, Coord. Chem. Rev. 44 (1982) 83–126.
- [22] F. Wilkinson, W.P. Helman, A.B. Ross, J. Phys. Chem. Ref. Data 22 (1993) 113–262.
- [23] P.A. Firey, W.E. Ford, J.R. Sounik, M.E. Kenney, M.A.J. Rodgers, J. Am. Chem. Soc. 110 (1988) 7626–7630.
- [24] W.P. Tood, J.P. Dinnocenzo, S. Farid, J.L. Goodman, I.R. Gould, J. Am. Chem. Soc. 113 (1991) 3601–3602.
- [25] O. Hammerich, in: H. Lund, O. Hammerich (Eds.), Organic Electrochemistry, Marcel Dekker, Inc., New York, 2001, pp. 95–182.
- [26] B.L. Wheeler, G. Nagasubramanian, A.J. Bard, L.A. Schechtman, D.R. Dinny, M.E. Kenney, J. Am. Chem. Soc. 106 (1984) 7404–7410.
- [27] H. Dreeskamp, E. Koch, M. Zander, Ber. Bunsen. Ges. Phys. Chem. 78 (1974) 1328–1334.
- [28] H. Fernández, M.A. Zón, J. Electroanal. Chem. 332 (1992) 237–255.
- [29] M. Fujitsuka, A. Watanabe, O. Ito, K. Yamamoto, H. Funasaka, T. Akasaka, J. Phys. Chem. B 103 (1999) 9519–9523.
- [30] M. Fujitsuka, A. Watanabe, O. Ito, K. Yamamoto, H. Funasaka, J. Phys. Chem. A 101 (1997) 4840–4844.
- [31] S.L. Murov, I. Carmichael, G.L. Hug, Handbook of Photochemistry, 2nd ed., Marcel Dekker, New York, 1993.
- [32] P. Maruthamuthu, L. Venkatasubramanian, P. Dharmalingam, J. Chem. Soc., Faraday Trans. I 82 (1986) 359–363.
- [33] T. Shida, Electronic Absorption Spectra of Radical Ions, Elsevier Science Publishers, 1988.
- [34] R.A. Kipp, J.A. Simon, M. Beggs, H.E. Ensley, R.H. Schmehl, J. Phys. Chem. A 102 (1998) 5659–5664.
- [35] J. Mack, M.J. Stillman, Inorg. Chem. 36 (1997) 413–425.
- [36] J. Mack, M.J. Stillman, Coord. Chem. Rev. 219–221 (2001) 993–1032.
- [37] J.A. Lacey, D. Phillips, Phys. Chem. Chem. Phys. 4 (2002) 232–238.
- [38] J. Davila, A. Harriman, Photochem. Photobiol. 50 (1989) 29–35.
- [39] S.L. Mattes, S. Farid, J.C.S. Chem. Commun. (1980) 126–128.
- [40] S.L. Mattes, S. Farid, J. Am. Chem. Soc. 105 (1983) 1386–1387.
- [41] S.L. Mattes, S. Farid, J. Am. Chem. Soc. 108 (1986) 7356–7361.
- [42] M. Juliard, in: M.A. Fox, M. Chanon (Eds.), Photoinduced Electron Transfer, Elsevier, Amsterdam, 1988, pp. 217–313.
- [43] I.R. Gould, D. Ege, J.E. Moser, S. Farid, J. Am. Chem. Soc. 112 (1990) 4290–4301.
- [44] S. Nonell, J.W. Arbogast, C.S. Foote, J. Phys. Chem. 96 (1992) 4169–4170.
- [45] N. Rubio, J.I. Borrell, J. Teixidó, M. Cañete, A. Juarranz, A. Villanueva, J.C. Stockert, S. Nonell, Photochem. Photobiol. Sci. 5 (2006) 376–380.
- [46] I.R. Gould, J.E. Moser, B. Armitage, S. Farid, J. Am. Chem. Soc. 111 (1989) 1917–1919.
- [47] L. Ebersson, M.P. Hartshorn, O. Persson, J. Chem. Soc., Perkin Trans. 2 (1995) 1735–1744.
- [48] L. Ebersson, M.P. Hartshorn, O. Persson, F. Radner, Chem. Commun. (1996) 2105–2112.

- [49] L. Ebersson, M.P. Hartshorn, J.J. McCullough, O. Persson, F. Radner, *Acta Chem. Scand.* 52 (1998) 1024–1028.
- [50] L. Evans III, G. Patonay, *Talanta* 48 (1999) 933–942.
- [51] D. Gonzalez-Rodriguez, T. Torres, D.M. Guldi, J. Rivera, M.A. Herranz, L. Echevoyen, *J. Am. Chem. Soc.* 126 (2004) 6301–6316.
- [52] T. Nyokong, Z. Gasyna, M.J. Stillman, *Inorg. Chem.* 26 (1987) 1087–1095.
- [53] E. Ough, Z. Gasyna, M.J. Stillman, *Inorg. Chem.* 30 (1991) 2301–2310.
- [54] T. Niwa, C. Sato, K. Kikuchi, M. Yamauchi, T. Nagata, Y. Takahashi, H. Ikeda, T. Miyashi, *J. Am. Chem. Soc.* 121 (1999) 7211–7219.